Bioresource Technology 360 (2022) 127642

Contents lists available at ScienceDirect

Bioresource Technology

journal homepage: www.elsevier.com/locate/biortech

Enhanced methane production kinetics by graphene oxide in fed-batch tests

Michele Ponzelli [a,b,c], Jelena Radjenovic [a,d], Jörg E. Drewes [c], Konrad Koch [c,*]

[a] Catalan Institute for Water Research (ICRA), Emili Grahit 101, Girona 17003, Spain
[b] University of Girona, Girona 17003, Spain
[c] Chair of Urban Water Systems Engineering, Technical University of Munich, Am Coulombwall 3, Garching 85748, Germany
[d] Catalan Institution for Research and Advanced Studies (ICREA), Passeig Lluís Companys 23, Barcelona 08010, Spain

HIGHLIGHTS

- The impact of graphene oxide in a systematic fed-batch study was assessed.
- First-order and modified Gompertz models were applied to two model substrates.
- Positive graphene oxide impact on kinetics is visible only from feed II or III.
- Graphene oxide levels above 10 mg_{GO}/g_{VS} significantly improve methane kinetics.
- Application of graphene oxide is promising for highly degradable substrate.

GRAPHICAL ABSTRACT

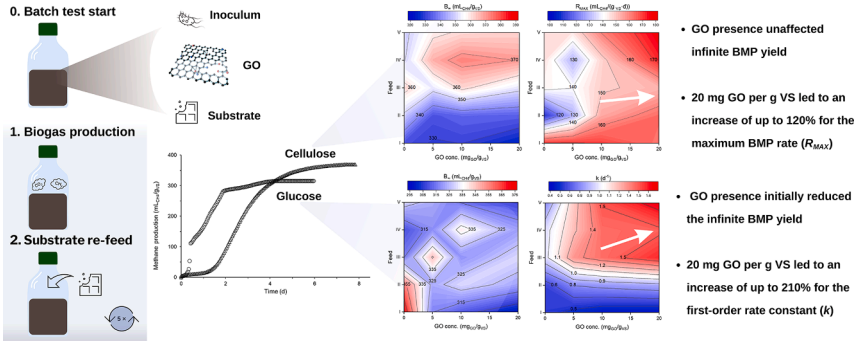

ARTICLE INFO

Keywords:
Anaerobic digestion
Graphene oxide
Methane production kinetics
Modeling
Biochemical methane potential tests

ABSTRACT

The study aims to prove that the addition of graphene oxide (GO) improves anaerobic digestion (AD) kinetic performance. Classical batch tests were modified to a fed-batch strategy at four GO levels while using two substrates (glucose and microcrystalline cellulose (MCC)). First-order and modified Gompertz models were respectively applied to evaluate the kinetic performance. The results showed significantly ($p < 0.05$) improved kinetic from the third refeeding step for both substrates. 20 mg GO per g of volatile solids (VS) led to an increase of up to 210% for the first-order rate constant (k) and up to 120% for maximum biochemical methane potential (BMP) rate (R_{MAX}) compared to control for glucose and MCC, respectively. The findings of this work suggest the implementation of GO in continuously operated systems to accelerate the AD process.

1. Introduction

Climate and recent geopolitical events are dictating the agenda of European governance towards a rapid transition in its energy source suppliers. Switching from fossil fuel consumption to renewables is leading the debates both at a climate change level, to meet the stringent greenhouse gas reduction target, and at the economic and energetical level to cope with the skyrocketing gas prices and to gain own energy independence (European Commission, 2022; European Commission, 2020). Biomethane production from anaerobic digestion (AD) of biodegradable materials, such as sewage sludge and the organic fraction of municipal waste, could play a crucial role in this transition. However,

* Corresponding author.
E-mail address: k.koch@tum.de (K. Koch).

https://doi.org/10.1016/j.biortech.2022.127642
Received 30 May 2022; Received in revised form 13 July 2022; Accepted 14 July 2022
Available online 18 July 2022

Table 1
Summary of the experimental conditions and their codes.

	GO conc. (mg_{GO}/g_{VS})			
Substrate	0	5	10	20
None	Blank	–	–	–
MCC	C-0	C-5	C-10	C-20
Glucose	G-0	G-5	G-10	G-20

Table 2
Description of the adopted kinetic models.

Model	Parameters	References
First-Order One-Step $B(t) = B_\infty(1 - e^{-kt})$	B_∞ = Infinite BMP yield (mL/g) k = First-order rate constant (1/d) t = Time (d)	(Angelidaki et al., 2009) (Brulé et al., 2014)
Modified Gompertz $B(t) = B_\infty \cdot e^{-e^{\left(\frac{R_{MAX}\cdot e}{B_\infty}(\lambda - t) + 1\right)}}$	B_∞ = Infinite BMP yield (mL/g) R_{MAX} = Maximum BMP rate (mL/g/d) λ = Lag time (d) t = Time (d)	(Zwietering et al., 1990)

one of the main drawbacks of the anaerobic treatment process is the relatively slow ability to transform complex substrates into biogas. The anaerobic process is indeed rate-limited by the successful syntropy of the two main constituting microbial communities, the fermenters and the methanogens (Cheng and Call, 2016). Their interactions and the successful production of the final product (i.e., methane and carbon dioxide) are intrinsically dependent on the interspecies electron transfer (IET) occurring among them (Baek et al., 2018). A possible way to increase the IET efficiency is switching to direct IET (DIET) by introducing conductive materials into the mixed liquor (Yin et al., 2020; Zhao et al., 2020). Different studies report significant enhancement of AD performance for different generally carbon-based amended materials, such as biochar (Wang et al., 2018), activated carbon (Yang et al., 2017), and nano-graphene materials (Wang et al., 2021).

Notably, results for graphene materials are conflicting. For example, Dong et al. (2019) documented a 7% and 12.6% methane production inhibition for graphene oxide (GO) with 54 and 108 mg of GO per gram of volatile solids (VS) in the inoculum (mg_{GO}/g_{VS}) during waste-activated sludge digestion. Similarly, Zhang et al. (2017) recorded inhibition from 2% to 17% with 0.155 to 15.5 mg_{GO}/g_{VS} for swine manure. On the other hand, an improvement of 17.6% in the cumulative methane yield was noticed during the co-digestion of sewage sludge and food waste when 1.1 g_{GO}/g_{VS} was added (Wang et al., 2021). Even Kundu et al. (2022) reported a 1.35-fold increase for 13.7 g_{GO}/g_{VS} addition in the AD of lemon waste.

The controversial results for GO addition in AD systems might be explained by the occurrence of its reduction mediated by the microbial community. The biological reduction of GO is a prerequisite for achieving DIET-related enhancement (Virdis and Dennis, 2017). Once GO undergoes such a reduction process, its defects, represented by the presence of oxygen functional groups, can indeed be partially restored through microbial respiration (Pei and Cheng, 2012; Salas et al., 2010). Thus, it is hypothesized that such DIET-related enhancement can be observed only at the 1 + refeeding step. For example, in Ponzelli et al. (2022), although the biological reduction of GO under anaerobic conditions occurred, the expected improvement of the biogas production was not observable. It was assumed that the microbial community needs a certain time to adapt to the additive, while the additive may also consume electrons during its bioreduction, making them not available for methane formation. Therefore, the initially limited methane production is based on three potential reasons: i) the biological reduction of GO consumes electrons from the supplied substrate, which would otherwise be available for methane production (Bueno-López et al., 2020); ii) introduction of the nanomaterial acts initially as an environmental stressor, causing the inhibition of bacterial activity including cell death, wrapping, and trapping (Zhang et al., 2017); or iii) high adsorption properties of the graphene material might also contribute to lower cumulative methane production, because the soluble organic matter might be adsorbed, and is thus less available for methane production (Dong et al., 2019). Such negative impacts on the anaerobic culture seem thus to be limited to the initial phase only when GO is amended for the first time. Extending the investigation period by subsequentially refeeding the batch reactors (or choosing a continuously operated system) would provide the necessary time to the anaerobic culture for adaptation to the additive and to turn the stressor into a stimulator. Moreover, antimicrobial properties of GO seem to be linked to oxidative mechanisms present only for small size GO sheets (Perreault et al., 2015). Contrarily, no bacterial inactivation for suspended growth systems was reported, but only cell trapping with impermanent effects.

In this study, the feeding strategy has been modified to simulate continuously fed reactors in batch experiments by applying multiple refeeds once the plateau phase of biogas production is reached (Font and

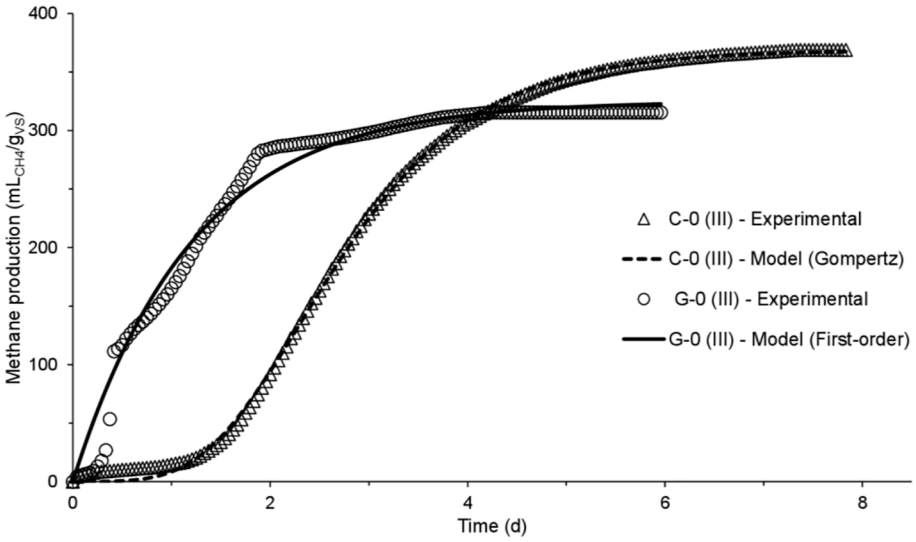

Fig. 1. Mean experimental values (symbols) and model data (line) of methane production for positive control of cellulose (C-0) and glucose (G-0) during feed III.

Table 3
Experimental, and kinetic parameters obtained from first-order one-step model for assays supplied with glucose. To evaluate the goodness of fit, the coefficient of determination (R^2) and the relative root mean square error (rRMSE) are also indicated. Standard deviation of five replicates is reported (n = 5), if not indicated differently (†: n = 4, ‡: n = 3).

			Model data			
		Experimental SMP	Glucose – First-order one-step		Model fit	
Sample	Feed	(mL_{CH4}/g_{VS})	B_∞ (mL_{CH4}/g_{VS})	k (1/d)	R^2 (-)	rRMSE (%)
G-0	I†	360.6 ± 12.2	372 ± 0	0.56 ± 0.04	0.98 ± 0.00	5.6 ± 0.6
	II	334.6 ± 5.7	358 ± 6	0.58 ± 0.02	0.98 ± 0.00	5.6 ± 0.6
	III†	311.6 ± 7.1	314 ± 8	0.96 ± 0.10	0.97 ± 0.01	5.5 ± 0.6
	IV†	301.8 ± 9.2	308 ± 4	0.96 ± 0.11	0.98 ± 0.01	3.8 ± 0.8
	V†	304.7 ± 12.7	329 ± 7	0.76 ± 0.08	0.98 ± 0.00	5.1 ± 0.4
G-5	I	289.6 ± 6.4	315 ± 5	0.49 ± 0.03	0.97 ± 0.00	6.6 ± 0.1
	II	331.6 ± 15.9	322 ± 16	0.76 ± 0.06	0.97 ± 0.01	6.7 ± 0.8
	III	349.6 ± 19.4	346 ± 16	1.33 ± 0.06	0.97 ± 0.00	4.5 ± 0.5
	IV	324.3 ± 6.0	318 ± 5	1.22 ± 0.06	0.98 ± 0.00	3.7 ± 0.2
	V	315.9 ± 8.2	322 ± 9	1.19 ± 0.05	0.98 ± 0.00	5.0 ± 0.6
G-10	I	277.8 ± 4.1	308 ± 4	0.44 ± 0.01	0.97 ± 0.00	7.0 ± 0.2
	II	318.6 ± 5.6	330 ± 7	0.80 ± 0.06	0.97 ± 0.01	6.1 ± 0.6
	III†	326.3 ± 7.3	317 ± 7	1.43 ± 0.09	0.98 ± 0.00	3.5 ± 0.2
	IV†	341.9 ± 16.1	339 ± 15	1.43 ± 0.05	0.99 ± 0.00	2.8 ± 0.2
	V	314.8 ± 3.3	314 ± 4	1.50 ± 0.10	0.99 ± 0.00	3.7 ± 0.7
G-20	I	266.2 ± 12.9	298 ± 12	0.42 ± 0.03	0.97 ± 0.00	7.6 ± 0.4
	II	311.4 ± 6.1	321 ± 10	0.84 ± 0.09	0.97 ± 0.00	5.7 ± 0.5
	III	334.1 ± 23.6	329 ± 20	1.57 ± 0.13	0.98 ± 0.00	3.1 ± 0.3
	IV	322.4 ± 8.9	319 ± 8	1.46 ± 0.07	0.99 ± 0.00	2.4 ± 0.3
	V†	308.1 ± 7.2	307 ± 5	1.65 ± 0.20	0.99 ± 0.00	3.3 ± 0.5

López Cabanes, 1995). Therefore, low-cost GO is added to anaerobic sludge to evaluate its impact on the degradation kinetics of two model substrates, glucose and microcrystalline cellulose (MCC), over multiple refeeds. Furthermore, the intrinsic difference between the two selected substrates may allow a better understanding of the stimulating/antagonistic effect of GO addition on the limiting step in the AD process. Glucose is known as an easily degradable material. No hydrolysis is needed and acidification is known to happen very fast, making it a substrate to identify potential impacts of GO addition on the methanogenesis step (Angelidaki et al., 2009). On the other hand, MCC degradation involves all the AD steps, with hydrolysis as its rate-limiting step (Holliger et al., 2016). Differentiating between these two substrates and comparing their performance allows the identification of which limiting step is favored or inhibited by the GO addition.

2. Materials and methods

2.1. Materials and chemicals

The GO was provided from Graphenea (San Sebastián, Spain) as a 4 g/L aqueous dispersion, with a flake size <10 μm. Powder MCC (CAS 9004-34-6) (Alfa Aesar, Karlsruhe, Germany) and D-glucose (CAS 50-99-7) (VWR International GmbH, Ismaning, Germany) were employed as model substrates.

2.2. Experimental setup and operation

Biochemical methane potential (BMP) experiments were carried out using three automatic methane potential test system II systems (AMPTS II, Bioprocess Control, Lund, Sweden). The experiments were conducted with glucose and MCC as substrates. The inoculum used in the experiments was collected from an anaerobic digester of the Garching wastewater treatment plant (Germany), working at mesophilic temperature (38 °C), treating a mixture of primary and secondary sludge. The inoculum was characterized by total solids (TS) and VS content of 19.5 ± 0.4 g_{TS}/kg and 12.3 ± 0.2 g_{VS}/kg (mean ± standard deviation, n = 3). For glucose and MCC, the TS content was 990.6 ± 0.6 g/kg and 998.5 ± 1.5 g/kg, respectively, and the VS/TS ratio was 100% in both cases. The inoculum substrate ratio (ISR) was set to 2 based on VS for both substrates, as recommended by the guidelines (Holliger et al., 2016). The operating conditions of the AMPTS are described elsewhere (Koch et al., 2020).

A factorial design with three factors and multiple levels was selected to perform the experiments. The factors are the type of substrate, the GO concentration (applied only at the beginning of the experiment), and the number of feeds. Table 1 outlines the employed levels for each factor.

All the tested conditions were conducted in quintuplicate (n = 5), including blanks (i.e., assays containing only inoculum), employed to determine the endogenous gas production from the inoculum itself. The working volume in each assay was only 250 mL (out of 500 mL total) because of observed overflow events in preliminary tests owing to the formation of hydrogel. Since the goal of this study was to evaluate the impact of GO during different feeds, the BMP termination criterion (i.e., <1% cumulative methane production over three consecutive days) was usually not achieved (Holliger et al., 2021). In contrast, an extended starvation period during the plateau phase is even assumed to be antagonistic to the activity of the microbial community. The refeed happened approximately every week for both substrates to avoid starvation, where only the substrate was added to the assays. It was hypothesized that the unavailability of the substrate could cause a longer lag-phase at the following refeed, altering the kinetic parameters provided by the models. A total of five subsequent feeds have been carried out and are indicated by roman numbers. Cumulative gas production was calculated by subtracting the endogenous methane production obtained from blanks. Blanks were run for the entire experimental period, without any opening or flushing between the different feeds.

2.3. Analytical methods

TS and VS of inoculum, glucose, and MCC were analyzed according to standard methods (Baird et al., 2017).

2.4. Kinetic models

Two kinetic models were adopted to estimate kinetic parameters based on the specific methane production (SMP) curve obtained from the AMPTS II (see Table 2). The first-order one-step model is commonly adopted to predict and assist operators in designing and operating full-scale plants (Veeken and Hamelers, 1999; Linke, 2006). It was selected here due to its simplicity and to gain insights into the kinetic constant.

The modified Gompertz model is a sigmoidal curve, initially used to

Table 4
Experimental, and kinetic parameters obtained from the modified Gompertz model for assays supplied with MCC. To evaluate the goodness of fit, the coefficient of determination (R^2) and the relative root mean square error (rRMSE) are also indicated. Standard deviation of five replicates is reported (n = 5), if not indicated differently (†: n = 4, ‡: n = 3).

			Model data				
		Experimental SMP	MCC – Modified Gompertz			Model fit	
Sample	Feed	(mL_{CH4}/g_{VS})	B_∞ (mL_{CH4}/g_{VS})	R_{MAX} ($mL_{CH4}/(g_{VS}\cdot d)$)	λ (d)	R^2 (-)	rRMSE (%)
C-0	I	332.8 ± 4.2	332 ± 4	170.4 ± 1.6	0.77 ± 0.03	1.00 ± 0.00	1.3 ± 0.1
	II	344.8 ± 5.9	349 ± 6	109.4 ± 5.9	1.40 ± 0.1	1.00 ± 0.00	0.8 ± 0.1
	III	364.0 ± 9.8	363 ± 11	142.3 ± 9.1	1.32 ± 0.09	1.00 ± 0.00	1.8 ± 0.6
	IV	353.3 ± 13.4	349 ± 16	146.0 ± 15.2	1.09 ± 0.16	1.00 ± 0.00	2.3 ± 1.0
	V	352.1 ± 11.7	348 ± 11	146.5 ± 21.7	0.94 ± 0.14	1.00 ± 0.00	2.5 ± 1.0
C-5	I	331.6 ± 10.3	329 ± 9	170.9 ± 5.3	0.73 ± 0.02	1.00 ± 0.00	1.2 ± 0.1
	II	333.1 ± 7.5	333 ± 7	128.7 ± 16.4	1.32 ± 0.04	1.00 ± 0.00	2.0 ± 1.1
	III†	353.9 ± 12.1	353 ± 11	140.2 ± 10.1	1.43 ± 0.17	1.00 ± 0.00	2.1 ± 0.5
	IV‡	365.6 ± 10.0	367 ± 16	129.5 ± 10.0	1.43 ± 0.15	1.00 ± 0.00	1.8 ± 0.4
	V	358.7 ± 9.8	358 ± 11	145.0 ± 20.8	1.09 ± 0.17	1.00 ± 0.00	2.2 ± 0.4
C-10	I	330.1 ± 5.1	330 ± 5	169.4 ± 2.8	0.69 ± 0.02	1.00 ± 0.00	1.1 ± 0.1
	II	345.4 ± 9.4	335 ± 8	154.7 ± 4.7	1.30 ± 0.11	1.00 ± 0.00	3.1 ± 0.8
	III†	367.6 ± 8.9	362 ± 13	148.8 ± 10.2	1.25 ± 0.12	1.00 ± 0.00	3.3 ± 1.1
	IV†	372.4 ± 10.1	373 ± 3	147.7 ± 11.5	1.27 ± 0.08	1.00 ± 0.00	3.1 ± 0.9
	V	364.8 ± 16.0	361 ± 17	160.3 ± 21.9	0.95 ± 0.15	1.00 ± 0.00	2.6 ± 0.4
C-20	I	326.6 ± 11.2	324 ± 10	162.5 ± 7.1	0.63 ± 0.03	1.00 ± 0.00	1.6 ± 0.1
	II	344.3 ± 19.2	334 ± 19	163.8 ± 13.7	1.19 ± 0.04	1.00 ± 0.00	2.7 ± 0.2
	III	359.5 ± 8.6	352 ± 8	152.6 ± 6.0	1.17 ± 0.10	1.00 ± 0.00	2.6 ± 0.6
	IV	375.7 ± 23.9	370 ± 25	172.3 ± 5.5	1.43 ± 0.24	1.00 ± 0.00	3.3 ± 0.5
	V	368.3 ± 19.1	362 ± 17	177.4 ± 35.2	0.94 ± 0.07	1.00 ± 0.00	2.8 ± 1.0

describe bacterial growth, consisting of a lag-phase, exponential phase, and a stationary phase (Zwietering et al., 1990). Compared to the first-order models, the Gompertz model describes those substrates that exhibit an initial phase with low or absent biogas production (i.e., lag phase), which is frequently reported for complex substrates as MCC (Ware and Power, 2017). Moreover, the Gompertz model can provide insights into the maximum methane production rate and the lag-phase duration. As for the first-order model, this obtainable information on rate constant and lag-phase duration is helpful to determine the synergistic or antagonistic effect of GO addition to anaerobic systems and compare GO-amended conditions with control ones or similar literature studies.

Initial iteration values are set according to indications by Brulé et al. (2014). All variables are constrained to non-negative values (≥0), and infinite BMP (B_∞) is constrained to the theoretical BMP of the corresponding substrate, i.e., values less than or equal to 372 and 414 mL_{CH4}/g_{VS} for glucose ($C_6H_{12}O_6$) and MCC ($(C_6H_{10}O_5)_n$), respectively.

2.5. Statistical parameters and analysis

Kinetic parameters were calculated through iteration using the MS Excel solver function. The objective function was set to minimize the relative standard square error (RSS). The relative root means square error (rRMSE) and the coefficient of determination R^2 were used to assess the model's fitness and efficiency (Weinrich and Nelles, 2021). Analysis of the residuals, i.e., the differences between experimental and model data, were also calculated to evaluate the closeness of the model to reality.

Moreover, a two-way analysis of variance (ANOVA) was carried out using Origin 2021 software (OriginLab Corporation, Northampton, Massachusetts, US) to evaluate statistical differences among the different experimental conditions, and values of $p < 0.05$ were considered significant.

3. Results and discussion

The study was conducted to systematically evaluate the impact of GO addition in batch tests following a fed-batch strategy. The results are divided into two sets according to the two different investigated substrates. The first set is focused on the experiments with glucose, where the first-order model is applied. The second set represents the results of the experiments with cellulose, where the modified Gompertz model is used. Moreover, a preliminary section on the goodness of the fit is presented.

3.1. Model efficiency

The main goal of this study was to evaluate the degradation kinetics of two model substrates with very different digestion behavior. Thus, two widely applied models have been chosen: the first-order one-step model for glucose and the modified Gomperz for MCC. As shown in Fig. 1, the first-order model fits well with the methane production curve from glucose degradation. The condition G-0 (III) serves as a representative example and shows a high R^2 of 0.98 and a low rRMSE of 4.9%, confirming the generally high goodness of the fit for glucose with the first-order model. Assay C-0 (III) for MCC modeled by modified Gompertz perfectly describes SMP curve with an R^2 of 1.0 and an rRMSE of only 1.5%. Very similar behavior was observed for the other tested conditions (see Table 3 and Table 4), confirming the appropriateness of the two selected models.

3.2. Effects of GO addition on the degradation kinetics of glucose

The first-order one-step model was applied to evaluate the kinetic parameters obtained from batch assays supplied with glucose. As illustrated in Fig. 2b, the GO presence initially reduced the infinite BMP yield B_∞ (i.e., during feed I and II). Otherwise, no differences between GO-amended assays and the control condition (G-0) for B_∞ were noticed during subsequent feedings. The limited methane yield in the first feeding events may be explained by the reported entrapment effect of

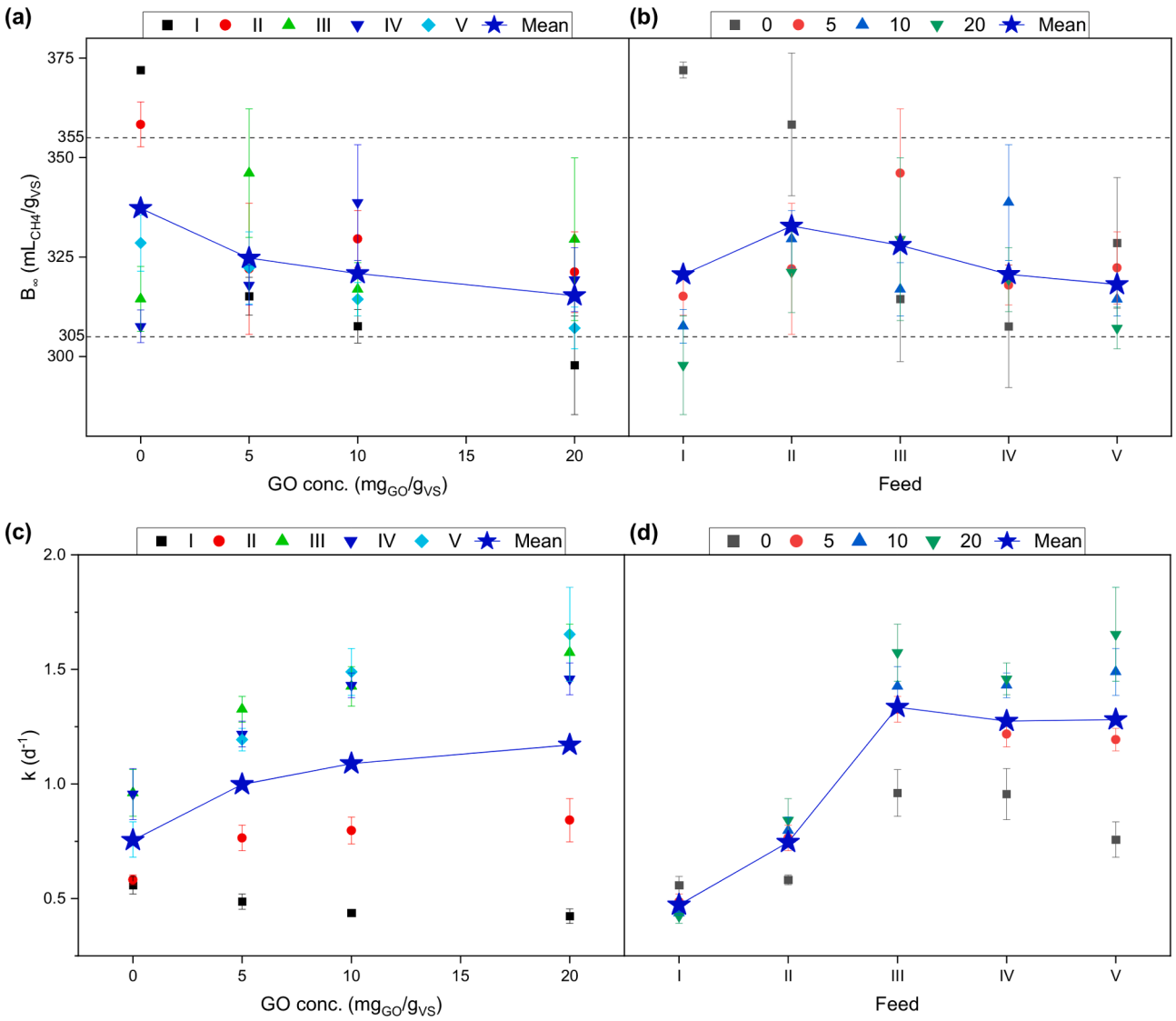

Fig. 2. Plots of each condition supplied with glucose during the five feeds and for the four GO levels (0, 5, 10, and 20 mg_{GO}/g_{VS}) for the infinite BMP yield B_∞ (**a**, and **b**), and the first-order rate constant *k* (**c**, and **d**). Star symbols indicate the mean of all assays for each abscissa position. Horizontal dotted lines in (**a**) and (**b**) stand for the refined validation criterion of 82.1% and 95.4% of the theoretical BMP of glucose (i.e., 372 mL_{CH4}/g_{VS}) from Holliger et al. (2021). Error bars represent standard deviation (n = 5).

the additive (Perreault et al., 2015). Previous studies also reported dose- and time-dependent cytotoxicity effects of graphene materials on bacterial communities (Guo et al., 2017; Liu et al., 2011). Thus, the trapping and toxic effects mitigate over time, resulting in similar B_∞ values across all conditions from feed III on.

In terms of the first-order degradation rate constant *k* (Fig. 2d), no impact was noticed during feed I and II. Instead, from feed III to V, all GO-amended assays (i.e., G-5, G-10, and G-20) showed values above 1.2 d^{-1}, significantly higher than G-0 (0.96–0.76 d^{-1}). Such findings might confirm the formulated hypothesis that digestion performance inhibition for GO-amended assays occurs only during initial periods. Thereafter, an improvement in degradation kinetics is apparent, with a comparable methane yield of control ranging between 308 and 329 mL_{CH4}/g_{VS}.

Although the BMP termination criteria were not fulfilled in most tests, it should be mentioned that the calculated infinite BMP yield B_∞ reached values in line with the reference value of 305–355 mL_{CH4}/g_{VS} (Fig. 2a and b), which represent the refined validation criterion of 82.1% and 95.4% of the theoretical BMP of glucose (i.e., 372 mL_{CH4}/g_{VS}) (Holliger et al., 2021). As illustrated in Fig. 2a and b, GO presence seems to affect B_∞ during feed I negatively. After that, GO-added assays achieved B_∞ values comparable to the control condition. One unexpected finding is the high B_∞ of 372 ± 0 mL_{CH4}/g_{VS} (corresponding to the upper model constraint) obtained for G-0 during feed I. A similar observation has been reported by Koch et al. (2017) for cellulose. The authors concluded that residual organic matter in the inoculum was degraded in the assay with substrate owing to an improved C/N ratio by adding carbon-rich substrate, while this was not the case in the inoculum-only assay.

From Fig. 2d, it is evident how higher degradation kinetics were achieved from feed III on for GO-supplied assays, while the control condition (i.e., G-O) exhibited significantly lower values. Moreover, considering the trend of the mean values (stars signs) of Fig. 2c, a maximum for *k* is obtained for GO concentrations even higher than 20 mg_{GO}/g_{VS}. However, considering each feed, two-way ANOVA showed that G-10 is not performing significantly different from G-20, but was significantly different from G-5 (until feed III). Thus, even a concentration of 10 mg_{GO}/g_{VS} is enough to achieve significantly faster degradation.

The findings from this section suggest a stimulating role of GO in

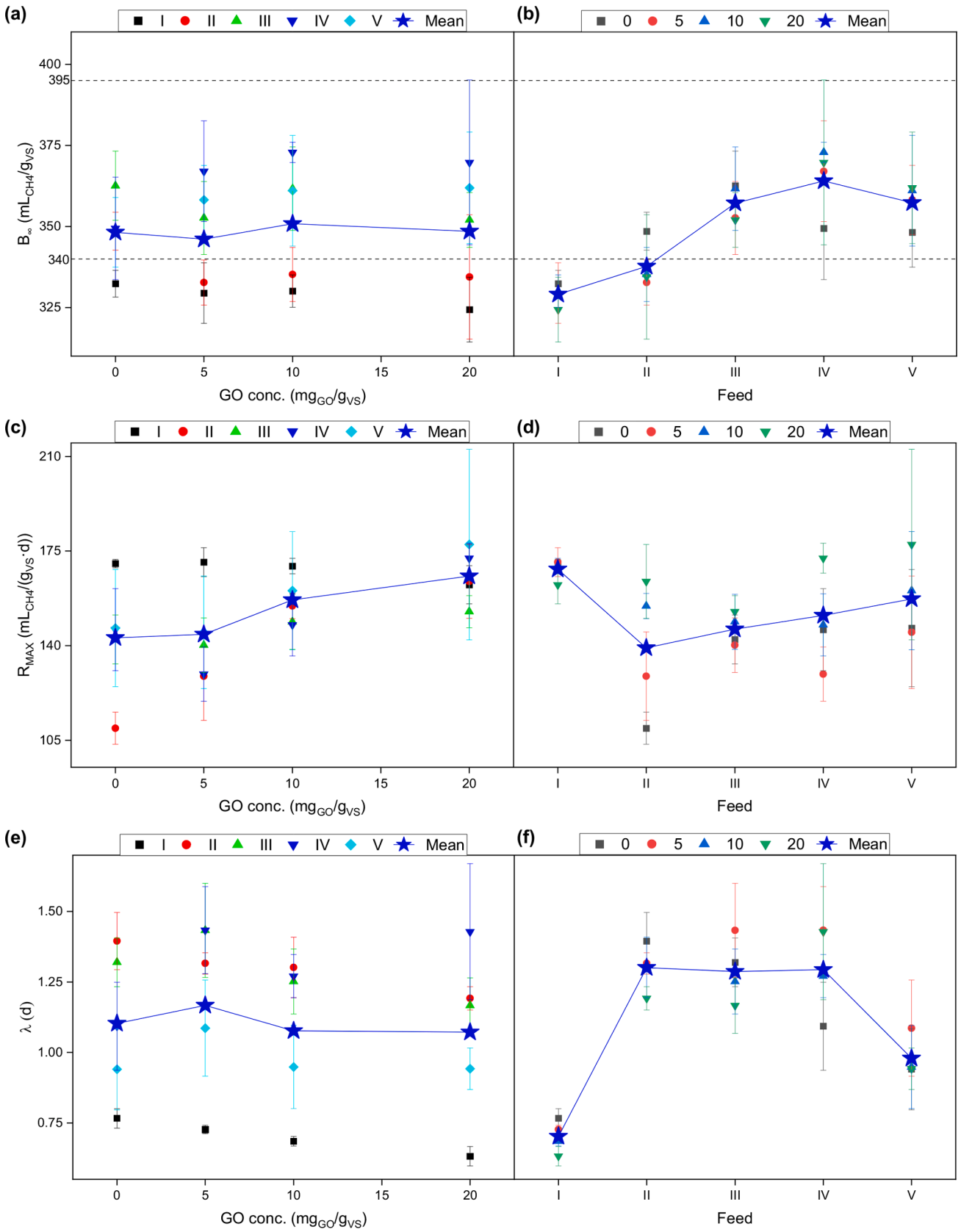

Fig. 3. Plots of each condition supplied with MCC during the five feeds and for the four GO levels (0, 5, 10, and 20 mg_{GO}/g_{VS}) for the infinite BMP yield B_∞ (**a**, and **b**), the maximum BMP rate R_{MAX} (**c**, and **d**), and the lag-phase length λ (**e**, and **f**). Star symbols indicate the mean of all assays for each abscissa position. Horizontal dotted lines in (**a**) and (**b**) stand for the refined validation criterion of 82.1% and 95.4% of the theoretical BMP of MCC (i.e., 414 mL_{CH4}/g_{VS}) from Holliger et al. (2021). Error bars represent standard deviation (n = 5).

promoting AD performance in fed-batch systems using easily degradable feedstock, like glucose.

3.3. Effects of GO addition on the degradation kinetics of cellulose

Experimental results of methane production obtained with MCC-supplied assays were simulated using the modified Gompertz model. Fig. 3a showed that regardless of the GO level applied, the infinite BMP yield B_∞ was statistically unaffected during each feed, varying from about 324 to 373 mL_{CH4}/g_{VS}. There was no initial inhibition of GO-amended tests for MCC-supplied assays compared to glucose. Thus, the initial inhibition may not be attributed to the bioreduction of GO consuming some of the electrons only, but probably to other underlying mechanisms. For instance, the hydrolysis of MCC is carried out by the synergetic reactions of microbial secreted endo- and *exo*-enzymes (α-amylase and oligo-1,6-glucosidase), not involved in glucose degradation (Fujii and Shimizu, 1986). The rate-limiting step defines the kinetics of methane formation. For glucose, this is likely the methanogenesis, and the methanogens seem to be inhibited by the presence of GO initially. In contrast, the rate-limiting step for MCC is hydrolysis performed by bacteria, which do not seem to be negatively impacted by the GO.

On the other hand, the maximum BMP rate R_{MAX} was significantly improved when a GO concentration higher than or equal to 10 mg_{GO}/g_{VS} was added to the system (Fig. 3c). It is important to remark that R_{MAX} has a lower kinetic explanatory power than *k* of the first-order model, which is determined from the slope of all data points, while R_{MAX} is the single point of maximum methane production. It is, however, interesting to observe that condition C-5 showed both lower R_{MAX} and longer lag-phase duration λ, indicating an antagonistic impact of low GO concentration (i.e., 5 mg_{GO}/g_{VS}) on methane formation (Fig. 3c and e). At the same time, this was not valid for the corresponding condition with glucose: G-5. This finding is consistent with Zhang et al. (2017), who found a greater inhibition of methane production at low GO levels (5 mg/L).

From Fig. 3b, a rising trend of B_∞ during the subsequent feeds is visible, which ultimately reached a stable value from feed III on. Likely, microorganisms adapted to the same substrate supplied over time (Koch et al., 2017). A nitrogen inhibition due to low C/N in the inoculum sample might also be accounted for interpreting the higher R_{MAX} noticed during feed I (Fig. 3d) (Wang et al., 2014). Overall, higher R_{MAX} values were found at higher GO concentrations (Fig. 3c). This finding aligns well with a previous observation of Lin et al. (2018), who found a linear correlation between kinetic parameters and the applied graphene concentration. Even Quintana-Najera et al. (2022) noticed a significant increase of R_{MAX} for increasing biochar addition during the co-digestion of cellulose and *Chlorella vulgaris*. Both additives, graphene and biochar, are also carbon-based and known to promote DIET. In contrast, Zhang et al. (2017) found a bell-shaped methane production inhibition over 0.6–16 mg_{GO}/g_{VS}. The statistical analysis carried out for this study revealed that at least an amount of 10 mg_{GO}/g_{VS} is needed to achieve a significantly higher R_{MAX} than the control. Besides, conditions C-10 and C-20 do not show any significant difference for each feed. Therefore, the 10 mg_{GO}/g_{VS} level might be a possible optimum for R_{MAX} improvement. However, the extension of GO concentration to values greater than 20 mg_{GO}/g_{VS} is needed to verify such a claim and to check whether an inhibition may occur at higher GO amounts.

Regarding the lag-phase duration λ, except for point C-20 during feed V, which has a p-value of 0.038 (close to the selected one of 0.05), a significant difference among the four tested GO levels was absent (Fig. 3e). Hence, no apparent impact of GO was noticed on the lag-phase duration. Contrarily, highly significant differences can be noticed between feed I (i.e., 0.70 d) and the subsequent ones (i.e., feed II, III, IV, and V), which showed mean λ values of 1.30, 1.29, 1.29, and 0.98, respectively (Fig. 3f). A plausible explanation for such shorter λ during the I. feed might be the presence of undegraded substrate present in the inoculum. The higher R_{MAX} detected during feed I may also support this explanation (Fig. 3d).

3.4. Outlook

The adoption of the two models allowed the estimation of methane production kinetic emphasizing the beneficial effect of GO addition on the degradation kinetics of two different substrates. The experimental results revealed that GO concentration above 10 mg_{GO}/g_{VS} improved the kinetic parameters while showing no inhibitory effect on the methane yield compared to the control from 1 + refeeding steps.

The reported inhibition of the AD process was, in most cases, an observation of a one-time application that could be overcome in non-batch systems. The applied fed-batch system is quasi between a batch test and a continuously operating system. These promising results should culminate in continuous experiments with GO. Besides, further research may supply other (real) substrates, test higher GO concentrations (for some parameter could be beneficial), analyze the potential shift in the microbial community, or investigate intermediates products of AD. Enhancement in biogas production with the addition of GO to glucose assays may be a promising strategy for treating high-strength food-processing wastewaters like the sugar industry, characterized by a high content of rapidly-degradable organic material.

4. Conclusions

Fed-batch tests with glucose and MCC revealed that GO concentrations greater than or equal to 10 mg_{GO}/g_{VS} are critical for accelerating methane production rates. However, this improvement only occurs after 1 + feed steps. Overall, this study demonstrates that the addition of GO at low quantities can accelerate the AD process in fed-batch systems.

CRediT authorship contribution statement

Michele Ponzelli: Conceptualization, Methodology, Investigation, Data curation, Formal analysis, Visualization, Writing – original draft. **Jelena Radjenovic:** Writing – review & editing, Supervision. **Jörg E. Drewes:** Writing – review & editing, Supervision. **Konrad Koch:** Conceptualization, Visualization, Writing – review & editing, Supervision.

Declaration of Competing Interest

The authors declare that they have no known competing financial interests or personal relationships that could have appeared to influence the work reported in this paper.

Data availability

Data will be made available on request.

Acknowledgments

This work was supported by the European Union's Horizon 2020 research and innovation programme under the Marie Sklodowska-Curie grant agreement – MSCA-ITN-2018 (EJD Nowelties, grant number 812880).

References

Angelidaki, I., Alves, M., Bolzonella, D., Borzacconi, L., Campos, J.L., Guwy, A.J., Kalyuzhnyi, S., Jenicek, P., Van Lier, J.B., 2009. Defining the biomethane potential (BMP) of solid organic wastes and energy crops: A proposed protocol for batch assays. Water Sci. Technol. 59, 927–934. https://doi.org/10.2166/wst.2009.040.

Baek, G., Kim, J., Kim, J., Lee, C., 2018. Role and potential of direct interspecies electron transfer in anaerobic digestion. Energies 11 (1), 107.

Baird, R.B., Eaton, A.D., Rice, E.W., 2017. Standard Methods for the Examination of Water and Wastewater, 23rd ed. American Public Health Association. Washington, D.C.

Brulé, M., Oechsner, H., Jungbluth, T., 2014. Exponential model describing methane production kinetics in batch anaerobic digestion: A tool for evaluation of biochemical methane potential assays. Bioprocess Biosyst. Eng. 37, 1759–1770. https://doi.org/10.1007/s00449-014-1150-4.

Bueno-López, J.I., Nguyen, C.H., Rangel-Mendez, J.R., Sierra-Alvarez, R., Field, J.A., Cervantes, F.J., 2020. Effects of graphene oxide and reduced graphene oxide on acetoclastic, hydrogenotrophic and methylotrophic methanogenesis. Biodegradation 31, 35–45. https://doi.org/10.1007/s10532-020-09892-0.

Cheng, Q., Call, D.F., 2016. Hardwiring microbes: Via direct interspecies electron transfer: Mechanisms and applications. Environ. Sci. Process. Impacts 18, 968–980. https://doi.org/10.1039/c6em00219f.

Dong, B., Xia, Z., Sun, J., Dai, X., Chen, X., Ni, B.J., 2019. The inhibitory impacts of nano-graphene oxide on methane production from waste activated sludge in anaerobic digestion. Sci. Total Environ. 646, 1376–1384. https://doi.org/10.1016/j.scitotenv.2018.07.424.

European Commission. 2022. REPowerEU: Joint European Action for more affordable, secure and sustainable energy.

European Commission. 2020. Circular Economy Action Plan. #EUGreenDeal 4. https://doi.org/10.2775/855540.

Font, R., López Cabanes, J.M., 1995. Fermentation in fed-batch reactors-Application to the sewage sludge anaerobic digestion. Chem. Eng. Sci. 50, 2117–2126. https://doi.org/10.1016/0009-2509(95)00058-D.

Fujii, M., Shimizu, M., 1986. Synergism of endoenzyme and exoenzyme on hydrolysis of soluble cellulose derivatives. Biotechnol. Bioeng. 28, 878–882. https://doi.org/10.1002/bit.260280615.

Guo, Z., Xie, C., Zhang, P., Zhang, J., Wang, G., He, X., Ma, Y., Zhao, B., Zhang, Z., 2017. Toxicity and transformation of graphene oxide and reduced graphene oxide in bacteria biofilm. Sci. Total Environ. 580, 1300–1308. https://doi.org/10.1016/j.scitotenv.2016.12.093.

Holliger, C., Alves, M., Andrade, D., Angelidaki, I., Astals, S., Baier, U., Bougrier, C., Buffière, P., Carballa, M., De Wilde, V., Ebertseder, F., Fernández, B., Ficara, E., Fotidis, I., Frigon, J.C., De Laclos, H.F., Ghasimi, D.S.M., Hack, G., Hartel, M., Heerenklage, J., Horvath, I.S., Jenicek, P., Koch, K., Krautwald, J., Lizasoain, J., Liu, J., Mosberger, L., Nistor, M., Oechsner, H., Oliveira, J.V., Paterson, M., Pauss, A., Pommier, S., Porqueddu, I., Raposo, F., Ribeiro, T., Pfund, F.R., Strömberg, S., Torrijos, M., Van Eekert, M., Van Lier, J., Wedwitschka, H., Wierinck, I., 2016. Towards a standardization of biomethane potential tests. Water Sci. Technol. 74, 2515–2522. https://doi.org/10.2166/wst.2016.336.

Holliger, C., Astals, S., de Laclos, H.F., Hafner, S.D., Koch, K., Weinrich, S., 2021. Towards a standardization of biomethane potential tests: A commentary. Water Sci. Technol. 83, 247–250. https://doi.org/10.2166/wst.2020.569.

Koch, K., Hafner, S.D., Astals, S., Weinrich, S., 2020. Evaluation of common supermarket products as positive controls in biochemical methane potential (BMP) tests. Water 12, 1223. https://doi.org/10.3390/W12051223.

Koch, K., Lippert, T., Drewes, J.E., 2017. The role of inoculum's origin on the methane yield of different substrates in biochemical methane potential (BMP) tests. Bioresour. Technol. 243, 457–463. https://doi.org/10.1016/j.biortech.2017.06.142.

Kundu, D., Banerjee, S., Karmakar, S., Banerjee, R., 2022. A new insight on improved biomethanation using graphene oxide from fermented Assam lemon waste. Fuel 309, 122195. https://doi.org/10.1016/j.fuel.2021.122195.

Lin, R., Deng, C., Cheng, J., Xia, A., Lens, P.N.L., Jackson, S.A., Dobson, A.D.W., Murphy, J.D., 2018. Graphene Facilitates Biomethane Production from Protein-Derived Glycine in Anaerobic. Digestion. iScience 10, 158–170. https://doi.org/10.1016/j.isci.2018.11.030.

Liu, S., Zeng, T.H., Hofmann, M., Burcombe, E., Wei, J., Jiang, R., Kong, J., Chen, Y., 2011. Antibacterial activity of graphite, graphite oxide, graphene oxide, and reduced graphene oxide: Membrane and oxidative stress. ACS Nano 5, 6971–6980. https://doi.org/10.1021/nn202451x.

Pei, S., Cheng, H.M., 2012. The reduction of graphene oxide. Carbon N. Y. 50, 3210–3228. https://doi.org/10.1016/j.carbon.2011.11.010.

Perreault, F., De Faria, A.F., Nejati, S., Elimelech, M., 2015. Antimicrobial Properties of Graphene Oxide Nanosheets: Why Size Matters. ACS Nano 9, 7226–7236. https://doi.org/10.1021/acsnano.5b02067.

Ponzelli, M., Zahedi, S., Koch, K., Drewes, J.E., Radjenovic, J., 2022. Rapid Biological Reduction of Graphene Oxide: Impact on Methane Production and Micropollutant Transformation. SSRN Electron. J. 1–28 https://doi.org/10.2139/ssrn.4051222.

Quintana-Najera, J., Blacker, A.J., Fletcher, L.A., Ross, A.B., 2022. Influence of augmentation of biochar during anaerobic co-digestion of Chlorella vulgaris and cellulose. Bioresour. Technol. 343, 126086 https://doi.org/10.1016/j.biortech.2021.126086.

Salas, E.C., Sun, Z., Lüttge, A., Tour, J.M., 2010. Reduction of graphene oxide via bacterial respiration. ACS Nano 4, 4852–4856. https://doi.org/10.1021/nn101081t.

Virdis, B., Dennis, P.G., 2017. The nanostructure of microbially-reduced graphene oxide fosters thick and highly-performing electrochemically-active biofilms. J. Power Sources 356, 556–565. https://doi.org/10.1016/j.jpowsour.2017.02.086.

Wang, G., Li, Q., Gao, X., Wang, X.C., 2018. Synergetic promotion of syntrophic methane production from anaerobic digestion of complex organic wastes by biochar: Performance and associated mechanisms. Bioresour. Technol. 250, 812–820. https://doi.org/10.1016/j.biortech.2017.12.004.

Wang, P., Zheng, Y., Lin, P., Li, J., Dong, H., Yu, H., Qi, L., Ren, L., 2021. Effects of graphite, graphene, and graphene oxide on the anaerobic co-digestion of sewage sludge and food waste: Attention to methane production and the fate of antibiotic resistance genes. Bioresour. Technol. 339, 125585 https://doi.org/10.1016/j.biortech.2021.125585.

Wang, X., Lu, X., Li, F., Yang, G., Li, W., 2014. Effects of temperature and Carbon-Nitrogen (C/N) ratio on the performance of anaerobic co-digestion of dairy manure, chicken manure and rice straw: Focusing on ammonia inhibition. PLoS One 9 (5), e97265. https://doi.org/10.1371/journal.pone.0097265.

Weinrich, S., Nelles, M., 2021. Basics of Anaerobic Digestion – Biochemical Conversion and Process Modelling, DBFZ Report No. 40.

Yang, Y., Zhang, Y., Li, Z., Zhao, Z., Quan, X., Zhao, Z., 2017. Adding granular activated carbon into anaerobic sludge digestion to promote methane production and sludge decomposition. J. Clean. Prod. 149, 1101–1108. https://doi.org/10.1016/j.jclepro.2017.02.156.

Yin, Q., Gu, M., Wu, G., 2020. Inhibition mitigation of methanogenesis processes by conductive materials: A critical review. Bioresour. Technol. 317, 123977 https://doi.org/10.1016/j.biortech.2020.123977.

Zhang, J., Wang, Z., Wang, Y., Zhong, H., Sui, Q., Zhang, C., Wei, Y., 2017. Effects of graphene oxide on the performance, microbial community dynamics and antibiotic resistance genes reduction during anaerobic digestion of swine manure. Bioresour. Technol. 245, 850–859. https://doi.org/10.1016/j.biortech.2017.08.217.

Zhao, Z., Li, Y., Zhang, Y., Lovley, D.R., 2020. Sparking Anaerobic Digestion: Promoting Direct Interspecies Electron Transfer to Enhance Methane. Production. 23 (12), 101794.